
[View Journal Online](#)
[View Article Online](#)

Synthesis and *in vitro* drug release of primaquine phosphate loaded PLGA nanoparticles

Bharat Patel ^{*}, Satyendra Kumar Tripathi , Sandhya Pathak , Sandeep Shukla 
 and Archana Pandey 

Department of Chemistry, Dr. Harisingh Gour Vishwavidyalaya, Sagar 470003, India

bharatkp94@gmail.com (B.P.), tripathisatyendra829@gmail.com (S.K.T.), sandhyapathak935@gmail.com (S.P.), s.shukla3634@gmail.com (S.S.),
 prof.archanapandey@gmail.com (A.P.)

^{*} Corresponding author at: Department of Chemistry, Dr. Harisingh Gour Vishwavidyalaya, Sagar 470003, India.
 e-mail: bharatkp94@gmail.com (B. Patel).

RESEARCH ARTICLE



doi 10.5155/eurjchem.12.4.482-487.2138

Received: 06 July 2021
 Received in revised form: 27 September 2021
 Accepted: 27 October 2021
 Published online: 31 December 2021
 Printed: 31 December 2021

KEYWORDS

Drug release
 Nanoparticles
 Bioavailability
 Antimalarial drugs
 Plasmodium species
 Dynamic light scattering

ABSTRACT

Plasmodium falciparum is one of the most common resistant *Plasmodium* species responsible for high rates of morbidity and mortality in malaria patients. Clinical guidelines for the management of *Plasmodium falciparum* include the use of a dose of primaquine phosphate resulting intolerable side effects. Therefore, the aim of this work was to formulate primaquine phosphate-loaded PLGA nanoparticles by using a nanoprecipitation method in order to increase its bioavailability to minimize drug intake. This leads to reduced toxicity and better therapeutic efficacy of the drug. The synthesized nanoparticles were characterized by using dynamic light scattering (DLS), transmission electron microscopy (TEM), scanning electron microscopy (SEM), atomic force microscopy (AFM), Fourier transformed infrared spectroscopy (FTIR), differential scanning calorimetry (DSC), and powder X-ray diffraction (XRD). TEM analysis revealed the presence of smooth spherical-shaped nanoparticles. The drug DLS analysis confirmed the presence of negatively charged nanoparticles with particle size in the range of 100-400 nm. The drug release study was performed to analyses different kinetic models like zero-order model, first-order model, Higuchi model, Hixson-Crowell model, and Korsmeyer-Peppas model.

Cite this: *Eur. J. Chem.* 2021, 12(4), 482-487

Journal website: www.eurjchem.com

1. Introduction

Malaria is a fatal parasitic infection caused by the protozoan *Plasmodium*. Annually, approximately 220 million people worldwide are infected with malaria, resulting in approximately 411,000 deaths worldwide (WHO, 2020) [1]. *Plasmodium* species have developed resistance to different existing antimalarial drugs, thereby reducing the effectiveness of the current medication [2]. In addition, conventional formulations are nonspecific to intracellular parasites, hence higher dose is prescribed leading to intolerable tissue toxicity-related side effects [3]. Polymeric nanoparticles play a major role in modern novel drug delivery systems and have the ability to remove several drawbacks of conventional formulations. Nanoparticles have increased surface area and thus can improve the bioavailability of different drugs. They can also have high entrapment efficiency, specific site targeting abilities. Therefore, polymeric nano-formulations have better therapeutic efficacy and can decrease dose frequency due to the stability of release capabilities [4,5]. The nanoparticles generally have a hydrophobic internal core and a hydrophilic outer shell [6]. Several polymers have been exploited for the formulation of nano-

particles such as polylactic (PLA), polyglycolic acid (PGA), and poly(DL-lactide-coglycolide) copolymers (PLGA) because of their biodegradability, biocompatibility, and versatile degradation kinetics [7]. Amongst these polymers, PLGA is the most successfully used biodegradable polymer [8]. Many studies report the successful application of the PLGA polymer for the preparation of nanoparticles as drug carriers [9].

In this study, our focus is to prepare a PLGA nanoparticle formulation of primaquine phosphate (Figure 1), a highly effective antimalarial drug. Primaquine phosphate, an 8-aminoquinoline derivative, has the formula $C_{15}H_{27}N_3O_9P_2$ [10].

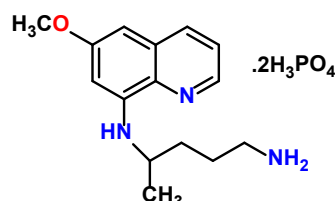


Figure 1. Chemical structure of primaquine phosphate.

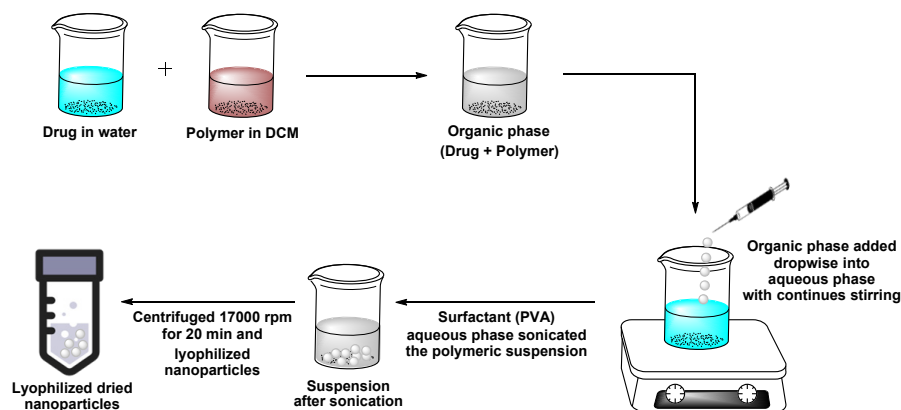


Figure 2. Schematic representation for the preparation of primaquine phosphate-loaded PLGA nanoparticles.

The development of primaquine-loaded solid lipid nanoparticles, galactose-anchored gelatin nanoparticles, PEGylated galactosylated nanolipid carrier, primaquine-loaded chitosan nanoparticles, etc. had never reported earlier [11-14]. However, primaquine phosphate-loaded PLGA nanoparticles have never been synthesized. In this work, we have prepared small-sized and less polydispersed primaquine phosphate loaded PLGA nanoparticles by using nanoprecipitation method. The *in vitro* drug release of the nanoparticle formulation was investigated using the dialysis bag method and the release behavior was analyzed using various kinetic models such as a zero-order model, first-order model, Higuchi model, Hixson-Crowell model, and Korsmeyer-Peppas model [15-17].

2. Experimental

2.1. Materials

Primaquine phosphate was gifted from Sun Pharma Laboratories Ltd., Gurgaon, Haryana, India. Poly (D-acid, L-lactic-co-glycol) (PLGA, 50:50, Mw: 30000-60000) was obtained from Sigma Aldrich, Bangalore, India. Polyvinyl alcohol (PVA, Mw: 160000, 86.5-89.0% hydrolyzed) are purchased from HiMedia Laboratories Pvt. Ltd., Nashik, India. Dichloromethane (DCM) were purchased from the Central Drug House (CDH), Delhi, India. Phosphate buffer, spam 80 were purchased from HiMedia Laboratory Pvt. Ltd., Mumbai, India. All solvents and chemicals were analytical grade.

2.2. Preparation of primaquine phosphate loaded PLGA nanoparticles

The formulation of drug-loaded PLGA nanoparticles was prepared by the modified nanoprecipitation method [18]. Briefly, a certain amount (10 mg) of drug dissolved in 2 mL of water and a certain amount (70 mg) of PLGA dissolved in 3 mL of dichloromethane solution. Aqueous phase was prepared by using 2 % of PVA (surfactant) solution having pH = 7.4 phosphate buffer saline. In the next step, the organic phase was added dropwise into the aqueous phase with a syringe under constant magnetic stirring at room temperature. Organic solvents were removed by continuous stirring overnight on a magnetic stirrer at 1200 rpm at room temperature. The formulation was sonicated under a bath sonicator (Bronson, Delhi, India) for 20 minutes at lower temperature. The nanoparticles were recovered by centrifugation at 17000 rpm for 15 minutes. The nanoparticles were washed twice with distilled water and then lyophilized. The final prepared nanoparticles were stored in a vacuum desiccator at 4 °C

[19,20]. The schematic representation of the preparation is given in Figure 2.

2.3. Particle size, zeta potential, and polydispersity index

The newly synthesized primaquine phosphate-loaded PLGA nanoparticles were released into deionized water. The suspension was characterized for particle size, zeta potential, and polydispersity index (PDI) by using the dynamic light scattering technique (DLS) (Malvern Instruments Ltd. and Nanoplus Particulated System).

2.4. Determination of drug entrapment efficiency and drug loading

The percentage of drug entrapment efficiency (%EE) and percentage of drug loading capacity (%DL) of synthesized nanoparticles was determined by following Equation (1) and (2) [21-23]. The freshly prepared suspension was centrifuged at 17000 rpm for 15 minutes to achieve a clear supernatant. The free drug in the supernatant was analyzed using a UV spectrometer (LABINDIA analytical, UV 3092) at 209 nm.

$$\%EE = \frac{\text{Total amount of drug} - \text{Free amount of drug in supernatant}}{\text{Total amount of drug}} \times 100 \quad (1)$$

$$\%DL = \frac{\text{Weight entrapped drug}}{\text{Weight of nanoparticles recovered}} \times 100 \quad (2)$$

2.5. Morphological analysis

The morphologies of the optimized PLGA loaded primaquine phosphate nanoparticles were studied by transmission electron microscope (TEM, TECNA), scanning electron microscope (SEM, NOVA NANO FESEM 450) and atomic force microscopy (AFM, INNOVA, ICON analytical equipment, Bruker). In the TEM analysis, the prepared nanoparticles were freeze dried and lyophilized. Freeze dried nanoparticles were then diluted with 2 mL of ethanol and evenly mixed by sonication for 5 min. The samples were prepared by placing a drop of the nanoparticle's suspension on the Formvar-coated copper grid and air dried. For the SEM analysis, the lyophilized nanoparticles were mounted onto double-sided adhesive carbon stubs, and the particles were viewed under low vacuum and high potential. The 3D organization and surface morphology of the nanoparticles were studied by AFM microscopy in tapping mode with 100 mm long spikes and cantilevered beams. The small amount of nanoparticle suspension was fixed to the magnetic study with the glass cover holder and dried at 50 °C in the oven.

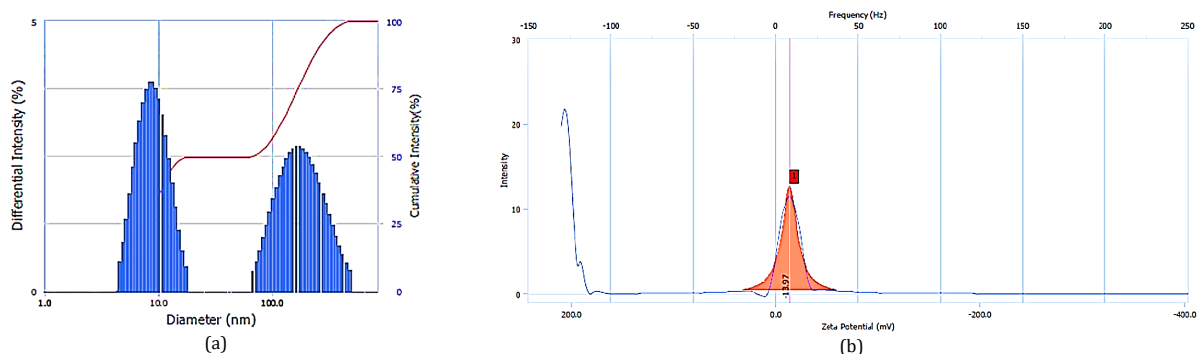


Figure 3. (a) Particle size distribution of nanoparticles and (b) Zeta potential of nanoparticles.

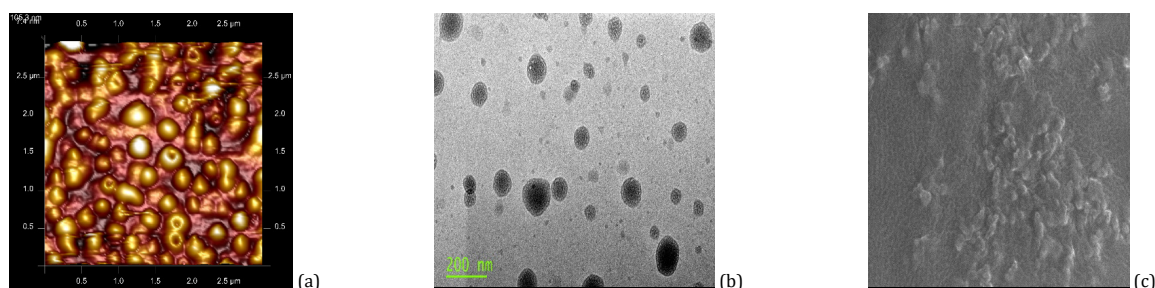


Figure 4. (a) 3D view of AFM of the formulation, (b) TEM image, and (c) SEM image of the nanoparticles.

2.6. Fourier transform infrared spectroscopy analysis

The FTIR spectra of PLGA, primaquine phosphate, and primaquine phosphate-loaded PLGA nanoparticles were recovered by using the Bruker-FTIR Spectrophotometer. The spectra were recovered in a wavelength range between 4000 and 400 cm^{-1} and interpreted with the help of FT-IR software.

2.7. Differential scanning calorimetry and thermal gravimetric analysis

To determine the differential scanning calorimetry curves of pure drugs and their PLGA nanoparticles, a DSC thermal analyzer was used. The crystalline nature of the medicinal product in the polymer matrix was evaluated. Thermal gravimetric analysis (TGA) determined the thermal stability of drug nanoparticle formulation. A sample of free drug and drug loaded PLGA nanoparticles thermograms was taken by using (NETZSCH): STA 449 F1 Jupiter connected to an inert stream of nitrogen gas and a heating rate of $10\text{ }^{\circ}\text{C}/\text{min}$ was used during the measurement.

2.8. Powder X-ray diffraction analysis

Powder X-ray diffraction patterns of pure drug, PLGA, polyvinyl alcohol, and drug-loaded PLGA nanoparticles were obtained by X-ray diffractometer (Bruker, D8-Advance) at room temperature in the range $10\text{--}80^{\circ}$ (2θ) at a scan rate of $4\text{ }^{\circ}\text{C}/\text{min}$. The evaluated powder samples were taken along the glass plate attached to the X-ray diffractometer.

2.9. In vitro drug release study and data analysis

An *in vitro* drug release study was conducted to determine the drug release profile by using primaquine phosphate-loaded PLGA nanoparticles. The *in vitro* release study was carried out using the dialysis bag method with the help of a dialysis membrane (Mw: 12000-14000 Da). Nanoparticles were placed in 10 mL of phosphate buffer (pH = 7.4) in dialysis bag at a

rotation speed of 100 rpm and temperature of $37\text{ }^{\circ}\text{C}$. Periodically, 5 mL of the sample was collected and the same volume of PBS (pH = 7.4) was added. The amount of drug released was determined by UV-VIS spectrometry analysis at wavelength of 209 nm at different times. The cumulative % drug released was analyzed by various kinetic models.

3. Results and discussion

3.1. Particle size, zeta potential, and polydispersity index

The size of the primaquine phosphate loaded PLGA nanoparticles was about $109\pm 3\text{ nm}$ (Figure 3), which was within the nano range. The PDI values of the nanoparticles were in the range of 0.483. The PDI value ≤ 1 showed that stability of the prepared nanoparticles. The zeta potential value was -13.97 mV . The negative values of zeta potential of the prepared nanoparticles could be attributed to functional group modification on the particle surface and ionic adsorption of the PLGA polymer.

3.2. Morphological analysis

The shape and surface morphology of the nanoparticles were identified by using AFM, TEM, and SEM techniques. The AFM image of nanoparticles formulation is shown in Figure 4a. However, TEM and SEM images of the formulation are shown in Figures 4b and c, respectively. The SEM and TEM images of primaquine phosphate loaded PLGA nanoparticles confirmed that the particle is spherical in shape, homogeneous size distribution and smooth. The analysis also indicates that the size of the nanoparticles is in the range of nano size and the diameter of the particle is $109\pm 3.18\text{ nm}$.

3.3. Determination of drug entrapment efficiency and drug loading

The entrapment efficiency of primaquine phosphate-loaded PLGA nanoparticles was calculated using the spectrophotometry

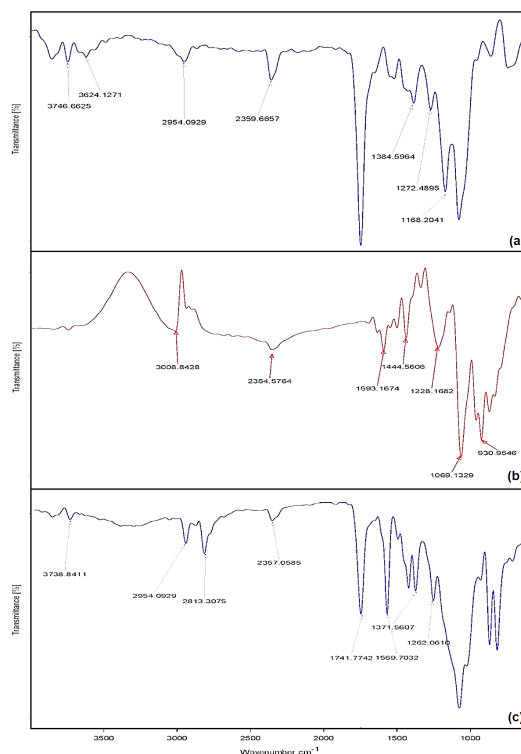


Figure 5. FTIR spectra of PLGA (a), primaquine phosphate (b), and primaquine phosphate loaded PLGA nanoparticles (c).

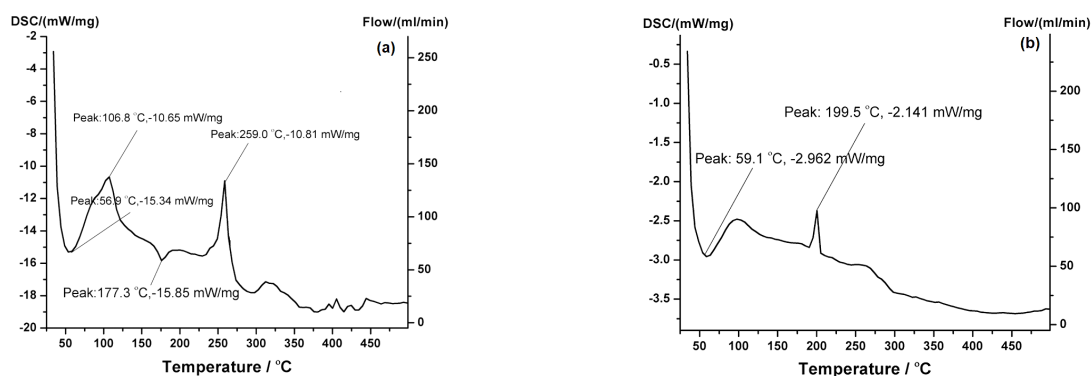


Figure 6. DSC of primaquine phosphate powder (a) and primaquine phosphate loaded PLGA nanoparticles (b).

metric method. The %EE and %DL of the primaquine phosphate-loaded PLGA nanoparticles were measured as 87 and 54%, respectively.

3.4. Fourier transform infrared spectroscopy (FT-IR) analysis

The FT-IR spectrum of primaquine phosphate, PLGA, and primaquine phosphate loaded PLGA nanoparticles is shown in Figure 5. The absorption bands in the spectra were recorded for the drug and its loaded PLGA nanoparticles in the 400-4000 cm^{-1} region.

FT-IR spectra of primaquine phosphate showed a characteristic peak of NH_2 bending at 1593 cm^{-1} , aromatic C=C stretching at 1445 cm^{-1} , C-N stretching at $1228, 1069 \text{ cm}^{-1}$. The spectra for PLGA polymer showed peaks at $3746\text{-}3624 \text{ cm}^{-1}$ which is its characteristic peak of O-H stretching. The C-H stretching peak was found at 2954 cm^{-1} , and the C-O stretching peaks at 1168 and 1272 cm^{-1} were also observed in the spectra. For primaquine phosphate loaded PLGA nanoparticles, the peaks of primaquine phosphate are much less intense due to the

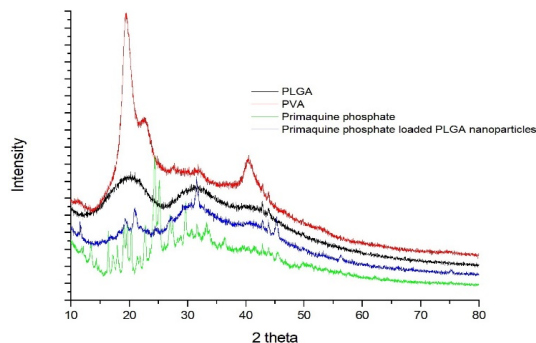
low concentration of the drug in the nanoparticles (Figure 5c). There is also no significant shift of functional peaks between the spectra of drugs, polymers and prepared nanoparticles. The spectral analysis indicated that the specific functional groups of polymeric material in the nanoparticles surface have almost the same chemical characteristics between the pure polymer and drug entrapped polymer.

3.5. DSC and TGA analysis

The study of thermal performance is a useful tool for the assessing whether drug particles have been encapsulated in polymeric matrices or not [24,25]. DSC determine the thermal stability of the drug and polymer formulation. Crystallinity of nanoparticles is a major factor because it significantly affects the solubility and dissolution properties of the drug. The DSC curve for pure primaquine phosphate is given in Figure 6a. The endothermic peak at $259.0 \text{ }^\circ\text{C}$ is corresponding to the melting point. Figure 6b shows the DSC curve of primaquine phosphate loaded PLGA nanoparticles.

Table 3. R² values and rate constants of different models for *in vitro* drug release studies.

No	Kinetic model	R ²	k	n
1	Zero-order	0.9693	1.24×10 ⁻¹	-
2	First-order	0.8530	6.80×10 ⁻³	-
3	Higuchi	0.9581	-	-
4	Hixson-Crowell	0.9090	1.30×10 ⁻³	-
5	Koersmeyer-Peppas	0.8972	1.24×10 ⁻¹	0.57

**Figure 7.** XRD spectrum of PLGA, PVA, primaquine phosphate, and PLGA loaded primaquine phosphate nanoparticles.

A strong endothermic peak was observed in primaquine phosphate loaded PLGA nanoparticles at 199.5 °C with a reduced intensity compared to pure primaquine phosphate. The shift in the endothermic peak is due to the loss of crystallinity that leads to the change in entropy of the drug due to its interactions with the polymer [26,27]. Primaquine phosphate evenly dispersed inside the PLGA polymer may have slow-release kinetics as desired. The degradation points of the analyzed samples were determined by the TGA analysis. The degradation of primaquine phosphate loaded PLGA nanoparticles starts at 60 °C and gradually degrades to above 250 °C [28,29]. This was comparable to that of free primaquine phosphate.

3.6. Powder X-ray diffraction analysis

The X-ray diffraction spectrum was taken for pure drug primaquine phosphate, PLGA, PVA, and primaquine phosphate loaded PLGA nanoparticles. The PVA peaks at 2θ position are 19.60, 22.60, 32.08, and 40.88° as shown in Figure 7. The PLGA polymer showed broad peaks at 2θ position 10-40° indicating its amorphous nature. The primaquine phosphate show peak at 2θ position θ 13.45, 16.63, 18.91, 19.95, 22.95, 24.71, 25.41, 27.17, 29.80, 31.73, 33.31, 36.49, and 42.98° due to its crystalline nature. Whereas, the primaquine phosphate loaded PLGA nanoparticles exist in amorphous state as shown in Figure 7. The primaquine phosphate in free form shows a crystalline nature, whereas the formulation shows an amorphous nature because the individual drug molecules are coated with PLGA polymer.

3.7. In-vitro drug release studies

The drug release studies were performed for the formulation, produced by modified nanoprecipitation method by using dialysis membrane. The formulation showed high entrapment efficiency and controlled release.

The release study was done upto 24 hours. The cumulative release of drug with different time interval were plotted in different kinetic models such as cumulative % of drug release with respect to time (Zero order kinetic model); log cumulative of % drug remaining with respect to time (First-order kinetic model); cumulative % drug release with respect to square root of time (Higuchi model); log cumulative % drug release with respect to log time (Korsmeyer-Peppas model).

The drug release rate constant (*k*) and correlation coefficients (*R*) obtained from different kinetic models are shown in Table 3. According to the best-fitted model, the maximum regression value (*R*²) is taken for consideration. It is concluded that the formulation follows the zero-order model, the correlation coefficient value of the zero-order model is 0.9693. The extent of the release exponent '*n*' in the Korsmeyer-Peppas model indicates that the release mechanism is non-Fickian diffusion.

4. Conclusions

Malaria is an illness that affects populations in tropical and subtropical countries. However, the recent development of nanomedicine is opening up new opportunities and providing better and more effective solutions to treat this complex disease. In this study, primaquine phosphate was successfully encapsulated into PLGA nanoparticles by nanoprecipitation method. Prepared nanoparticles showed desirable size and %EE to delay drug release, as confirmed by an *in vitro* dissemination study. Hence, it is concluded that the prepared nanoparticles benefit from the promise, better therapeutic efficacy and nanosized. Primaquine phosphate loaded PLGA nanoparticles can thus be a good alternative to conventional formulation with benefits of increased bioavailability, better patient compliance and decreased frequency of dose.

Acknowledgements

The author is grateful to University Grand Commission (UGC) for providing financial support. Authors are thankful to Harish Madan Sun Pharma Pharmaceuticals, Gurugram, Haryana for providing gift sample of drug API. We thank Dr. Vicky Mody, Associate Professor, Department of Pharmaceutical Sciences, Philadelphia College of Osteopathic Medicine (PCOM) School of Pharmacy, Suwannee, USA; Associate Professor for providing valuable suggestions in the whole work as and when required. The facilities provided by the Head, Department of Chemistry, and Head, Department of Pharmaceutical Science and Head Department of Microbiology, Dr. Harisingh Gour Vishwavidyalaya, Sagar (M.P.), are recognized as well. Author was thankful to Sophisticated Instrumentation Centre (SIC) for providing the facility of characterization and Department of Science and Technology-Promotion of University Research and Scientific Excellence (DST-PURSE)

Project for providing and chemicals, Dr. Harisingh Gour, Vishwavidyalaya, Sagar (M.P.).

Disclosure statement

Conflict of interests: The authors declare that they have no conflict of interest.

Ethical approval: There is no need of ethical approval in this manuscript.

Sample availability: Samples of the compounds are available from the author.

CRedit authorship contribution statement

Conceptualization: Bharat Patel, Archana Pandey; Methodology: Bharat Patel; Software: Bharat Patel; Validation: Bharat Patel, Satyendra Kumar Tripathi; Formal Analysis: Bharat Patel, Sandhya Pathak; Investigation: Bharat Patel; Resources: Bharat Patel; Data Curation: Bharat Patel; Writing - Original Draft: Bharat Patel; Writing - Review and Editing: Bharat Patel, Sandeep Shukla, Archana Pandey; Visualization: Bharat Patel; Funding acquisition: Bharat Patel; Supervision: Bharat Patel, Archana Pandey; Project Administration: Bharat Patel, Archana Pandey.

ORCID

Bharat Patel

 <https://orcid.org/0000-0002-2754-6965>

Satyendra Kumar Tripathi

 <https://orcid.org/0000-0001-5310-5461>

Sandhya Pathak

 <https://orcid.org/0000-0003-2516-8144>

Sandeep Shukla

 <https://orcid.org/0000-0001-6060-8251>

Archana Pandey

 <https://orcid.org/0000-0001-7974-2522>

References

- [1]. World Health Organization. *World Malaria Report 2019*; World Health Organization: Genève, Switzerland, 2019.
- [2]. Tripathy, S.; Das, S.; Chakraborty, S. P.; Sahu, S. K.; Pramanik, P.; Roy, S. *Int. J. Pharm.* **2012**, *434* (1–2), 292–305.
- [3]. Bagheri, A. R.; Golenser, J.; Greiner, A. *Eur. Polym. J.* **2020**, *129* (109625), 109625.

- [4]. Masiwa, W. L.; Gadaga, L. L. *J. Drug Deliv.* **2018**, *2018*, 3021738.
- [5]. Mangrio, F. A.; Dwivedi, P.; Han, S.; Zhao, G.; Gao, D.; Si, T.; Xu, R. X. *Mol. Pharm.* **2017**, *14* (12), 4725–4733.
- [6]. Urista, D. V.; Carru , D. B.; Otero, I.; Arrasate, S.; Quevedo-Tumaili, V. F.; Gestal, M.; Gonz lez-D az, H.; Munteanu, C. R. *Biology (Basel)* **2020**, *9* (8), 198.
- [7]. Surolia, R.; Pachauri, M.; Ghosh, P. C. *J. Biomed. Nanotechnol.* **2012**, *8* (1), 172–181.
- [8]. Kumari, A.; Yadav, S. K.; Yadav, S. C. *Colloids Surf. B Biointerfaces* **2010**, *75* (1), 1–18.
- [9]. Bohrey, S.; Chourasiya, V.; Pandey, A. *Nano Conver.* **2016**, *3* (1). <https://doi.org/10.1186/s40580-016-0061-2>.
- [10]. Gathirwa, J. W.; Omwoyo, W.; Ogotu, B.; Oloo, F.; Swai, H.; Kalombo, L.; Melariri, P.; Maroa, G. *Int. J. Nanomedicine* **2014**, *9* (1), 3865–3874.
- [11]. Gupta, N.; Rajera, R.; Nagpal, M.; Arora, S. *Pharm. Nanotechnol.* **2012**, *1* (1), 35–43.
- [12]. Kumar, H.; Gothwal, A.; Khan, I.; Nakhate, K. T.; Alexander, A.; Ajazuddin, Singh, V.; Gupta, U. *Mol. Pharm.* **2017**, *14* (10), 3356–3369.
- [13]. Baruah, U. K.; Gowthamarajan, K.; Ravisankar, V.; Karri, V. V. S. R.; Simhadri, P. K.; Singh, V.; Babu, P. P. *Artif. Cells Nanomed. Biotechnol.* **2018**, *46* (8), 1809–1829.
- [14]. Tripathy, S.; Mahapatra, S. K.; Chattopadhyay, S.; Das, S.; Dash, S. K.; Majumder, S.; Pramanik, P.; Roy, S. *Acta Trop.* **2013**, *128* (3), 494–503.
- [15]. Tiwari, R.; Aharwal, R. P.; Shukla, S.; Pandey, A. *Int. J. Pharm. Sci. Res.* **2014**, *5* (5), 1661–1670.
- [16]. Bohrey, S.; Chourasiya, V.; Pandey, A. *Polym. Sci. Ser. A* **2016**, *58* (6), 975–986.
- [17]. Baradaran Eftekhari, R.; Maghsoudnia, N.; Dorkoosh, F. A. *Expert Opin. Drug Deliv.* **2020**, *17* (3), 275–277.
- [18]. Salatin, S.; Barar, J.; Barzegar-Jalali, M.; Adibkia, K.; Kiafar, F.; Jelvehgari, M. *Jundishapur J. Nat. Pharm. Prod.* **2018**, *13* (4), e12873.
- [19]. Alshamsan, A. *Saudi Pharm. J.* **2014**, *22* (3), 219–222.
- [20]. Busari, Z. A.; Dauda, K. A.; Morenikeji, O. A.; Afolayan, F.; Oyeyemi, O. T.; Meena, J.; Sahu, D.; Panda, A. K. *Front. Pharmacol.* **2017**, *8*, 622.
- [21]. Haider, T.; Pandey, V.; Behera, C.; Kumar, P.; Gupta, P. N.; Soni, V. *J. Drug Deliv. Sci. Technol.* **2020**, *60* (102087), 102087.
- [22]. Kashi, T. S. J.; Eskandarion, S.; Esfandyari-Manesh, M.; Marashi, S. M. A.; Samadi, N.; Fatemi, S. M.; Atyabi, F.; Eshraghi, S.; Dinavand, R. *Int. J. Nanomedicine* **2012**, *7*, 221–234.
- [23]. Venkatesh, D. N.; Baskaran, M.; Karri, V. V. S. R.; Mannemala, S. S.; Radhakrishna, K.; Goti, S. *Saudi Pharm. J.* **2015**, *23* (6), 667–674.
- [24]. Ho, H. N.; Tran, T. H.; Tran, T. B.; Yong, C. S.; Nguyen, C. N. *J. Nanomater.* **2015**, *2015*, 1–12.
- [25]. Anwer, M. K.; Al-Mansoor, M. A.; Jamil, S.; Al-Shdefat, R.; Ansari, M. N.; Shakeel, F. *Int. J. Biol. Macromol.* **2016**, *92*, 213–219.
- [26]. Anwer, M. K.; Mohammad, M.; Ezzeldin, E.; Fatima, F.; Alalawi, A.; Iqbal, M. *Int. J. Nanomedicine* **2019**, *14*, 1587–1595.
- [27]. Izumikawa, S.; Yoshioka, S.; Aso, Y.; Takeda, Y. *J. Control. Release* **1991**, *15* (2), 133–140.
- [28]. Tripathy, S.; Das, S.; Chakraborty, S. P.; Sahu, S. K.; Pramanik, P.; Roy, S. *Int. J. Pharm.* **2012**, *434* (1–2), 292–305.
- [29]. Pan, X.; Liu, S.; Ju, L.; Xi, J.; He, R.; Zhao, Y.; Zhuang, R.; Huang, J. *Drug Dev. Ind. Pharm.* **2020**, *46* (11), 1889–1897.



Copyright © 2021 by Authors. This work is published and licensed by Atlanta Publishing House LLC, Atlanta, GA, USA. The full terms of this license are available at <http://www.eurjchem.com/index.php/eurjchem/pages/view/terms> and incorporate the Creative Commons Attribution-Non Commercial (CC BY NC) (International, v4.0) License (<http://creativecommons.org/licenses/by-nc/4.0>). By accessing the work, you hereby accept the Terms. This is an open access article distributed under the terms and conditions of the CC BY NC License, which permits unrestricted non-commercial use, distribution, and reproduction in any medium, provided the original work is properly cited without any further permission from Atlanta Publishing House LLC (European Journal of Chemistry). No use, distribution or reproduction is permitted which does not comply with these terms. Permissions for commercial use of this work beyond the scope of the License (<http://www.eurjchem.com/index.php/eurjchem/pages/view/terms>) are administered by Atlanta Publishing House LLC (European Journal of Chemistry).